Trapped electron modes in laser backscatter experiments

N. J. Sircombe
AWE plc. Aldermaston, Reading, Berkshire, RG7 4PR, UK
Centre for Fusion, Space and Astrophysics, Department of Physics, Warwick University, Coventry, CV4 7AL, UK
Central Laser Facility, CCLRC Rutherford Appleton Laboratory, Chilton, Didcot, Oxfordshire, OX11 0QX, UK

T. D. Arber
Centre for Fusion, Space and Astrophysics, Department of Physics, Warwick University, Coventry, CV4 7AL, UK

R. O. Dendy
UKAEA Culham Division, Culham Science Centre, Abingdon, Oxfordshire, OX14 3DB, UK
Centre for Fusion, Space and Astrophysics, Department of Physics, Warwick University, Coventry, CV4 7AL, UK

Main contact email address Nathan.Sircombe@awe.co.uk

Introduction

The consideration of non-Maxwellian particle distribution functions is a fundamental problem in plasma physics. Such distributions can, for example, allow the plasma to support a variety of modes often omitted from studies of Laser Plasma Interaction [1,2]. Both the electron acoustic wave (EAW) [3,4] and the beam acoustic mode (BAM) [5] have been identified as possible longitudinal daughter waves for stimulated scattering in plasmas [6,7,8]. Both modes permit oscillations below the plasma frequency, and so provide an additional mechanism for stimulated Raman-like scattering. Here we discuss the similarities and differences between the BAM and EAW, and highlight the difficulties in distinguishing between the modes. In doing this we hope to clarify earlier work on the electron acoustic wave [4] and summarise recent results [9]. We also outline fully nonlinear kinetic simulations which demonstrate both scattering from Langmuir waves and from modes with frequencies below the plasma frequency.

The electron acoustic and beam acoustic modes

Both BAMs and EAWs can be considered as modifications to a Maxwellian particle population that result in flattening about a particular velocity, as shown in figure 1. In the case of the EAW, the modification is an odd function about v_p given by

$$f_1(v) = \partial_v f_0\big|_{v_p}(v - v_p)\exp\left(\frac{-(v-v_p)^2}{\Delta v^2}\right) \qquad (1)$$

or similar, with an effective density of

$$\int f_1 dv = 0 \qquad (2)$$

This modifies the solutions to the Landau integral

$$\frac{1}{2(k\lambda_d)^2}\int_{-\infty}^{+\infty}\frac{\partial_v f(v)}{v-\omega/(kv_T)}dv \qquad (3)$$

in the conventional Langmuir dispersion relation to allow the propagation of EAWs. However, the BAM is supported by a beam added to the distribution at $v = v_b$. This beam is described by a function f_2 which is even about v_b and has an associated density given by

$$\int f_2 dv = n_2 \qquad (4)$$

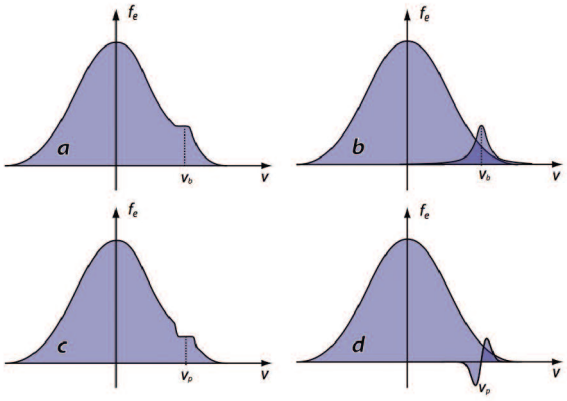

Figure 1. Distributions (a, c) which exhibit local flattening are able to support plasma modes such as the EAW and BAM. In the case of the BAM, the flattened distribution (a) is mathematically identical to (b), which comprises a background Maxwellian plus a smaller drifting electron distribution centred at v_b, produced via some acceleration mechanism. The Doppler shifted frequency of plasma oscillations supported by the drifting electron distribution produces oscillations below the plasma frequency in the rest frame of the system. In the case of the EAW, the flattened distribution (c) is the combination of a Maxwellian and a modification centred at v_p produced by the trapping of electrons (d) which does not contribute to the plasma density.

Rather than modifying the Landau solution, this beam admits a whole new branch of solutions.

In the frame of reference of the background population, oscillations at the electron plasma frequency supported by the beam population will be Doppler shifted by kv_b. As the beam density tends to zero, we obtain $\omega \sim v_b k$. This dispersion relation is linear in k for small k, and implies a frequency below the plasma frequency. A more complete derivation of the BAM dispersion relation is given by O'Neil *et al.* [3], for the case of both Lorentzian and Maxwellian beam distributions f_2, and yields the same result for small k. This description also raises the question of negative energy modes, which can be supported in similar beam-plasma systems [10]. Indeed, trapped electron modes similar to those described here can exist in a negative energy configuration [11], although not in the regime considered here.

The presence of an additional population of beam electrons allows the plasma to support a new mode, the BAM, at a phase velocity dictated by the beam velocity. The EAW, however, has a phase velocity prescribed by its dispersion relation. Flattening the distribution function at the correct velocity modifies the Landau integral and admits undamped solutions, the EAWs. The key difference between the BAM and the EAW is that the BAM requires an additional population with an associated mass and a finite drift velocity relative to the thermal background, while the EAW requires a distribution function flattened at a particular v, dictated by the dispersion relation. The physical processes at work are therefore different. BAMs require some form of acceleration mechanism to produce the beam population, whereas EAWs result from the trapping of electrons. However, it may be difficult to distinguish between the BAMs and EAWs, particularly for a low beam velocity.

Scattering from trapped particle modes

Non-Maxwellian particle distributions, which require a kinetic treatment of the plasma, can significantly affect the scattering of incident light [4,12], destroying the idealised picture of a three-wave parametric instability by allowing scattering from plasma oscillations omitted from conventional fluid treatments, such as the EAW and the BAM, described above. We now utilise a Vlasov-Maxwell code to investigate scattering from such modes and related kinetic effects in a regime close to that achieved in single hot-spot experiments [5,6]. This involves less than quarter critical densities (hence permitting SRS, in contrast to earlier work) [4,13] and the presence of a continuous EM driver.

The Vlasov solver introduced by Arber and Vann [13] and expanded in later work [4,14] was adapted for a system with a continuous, sinusoidal, EM driver and open boundaries. Any charge flowing past the system boundaries is assumed then to reside on a 'charged plate', external to the system. This external charge is included when calculating the electrostatic potential in order to avoid the creation of a DC field. The electrostatic potential is found using a tridiagonal matrix inversion, which in turn is used to calculate the electrostatic field.

The laser intensity I_0, electron temperature T_e and density n_e achieved in single hot-spot experiments [5,6] were, approximately:

$I_0 = 1.6\times10^{16}\mathrm{Wcm}^{-2}$

$T_e = 350\mathrm{eV}$

$n_e = 1.2\times10^{20}\mathrm{cm}^{-3} = 0.03n_c$

These imply values for the simulation parameters (incident EM wave amplitude E_y and frequency ω_0, thermal velocity v_{Te} and density n_e) of

$E_y = 0.33m_ec\omega_{pe}/e$

$\omega_0 = 5.7775\omega_{pe}$

$v_{Te} = 0.026c$

$n_e = 1\times\omega_{pe}^2\varepsilon_0/e^2 = 0.03n_c$

To minimise the charge loss from the system, a 'flat-top' density profile is used, where the density of both electrons and the neutralising ion background drops smoothly to zero over a distance $\sim 40c/\omega_{pe}$ at the edges of the system. The simulation domain extends from $x = 0$ to $x = 220c/\omega_{pe}$, leaving a flat region at the centre of the simulation box approximately $x = 140c/\omega_{pe}$ in length, and from $p = -0.75m_ec$ to $p = 0.75m_ec$. The simulation grid has 16,384 points in x and 1,024 points in p. The simulation runs to an end time of $1200/\omega_{pe}$.

Figures 2 and 3 display windowed Fourier transforms of the electrostatic field and of the back-propagating EM field, taken with a Hanning window of size $\sim 75/\omega_{pe}$, at the centre of the system. These show the development of low frequency plasma waves after $t = 600/\omega_{pe}$. In the initial SRS burst, starting at $t = 450/\omega_{pe}$ the EM driver at ω_0 scatters from a Langmuir wave at $\omega_1 = 1.06\omega_{pe}$, $k = 0.27/\lambda_D$, $v_p = 3.93vT_e$, to produce reflected light at a frequency $\omega_2 = 4.72\omega_{pe}$. This instability saturates via the trapping of electrons. Figure 4a shows the electron distribution function during the late stages of the SRS burst, when

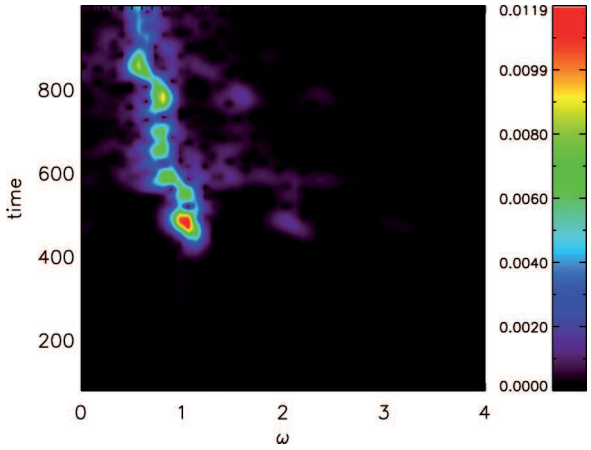

Figure 2. Windowed Fourier transform of the electrostatic field E_x at the centre of the system. An initial SRS burst saturates via the trapping of electrons which distort the initially Maxwellian distribution and provide an environment in which waves below the plasma frequency can grow and propagate. The traces at $\omega \approx 0.8\omega_{pe}$ and $\omega \approx 0.6\omega_{pe}$, first appearing at $t = 600/\omega_{pe}$, represent EAWs with phase velocities at $v_p = 2.73v_{Te}$ and $v_p = 2.03v_{Te}$.

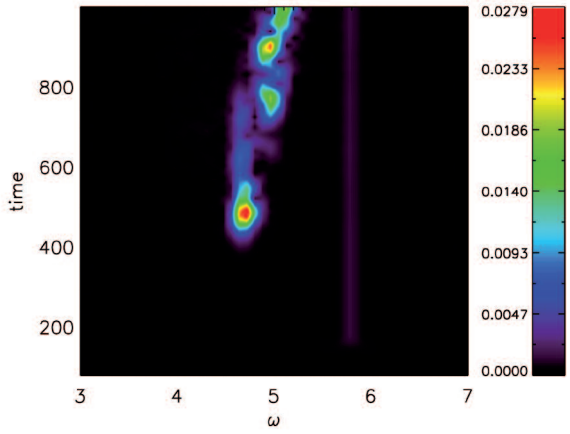

Figure 3. Windowed Fourier transform of the backwards propagating EM field at the centre of the system. The spectrum shows the light scattered by Langmuir waves (SRS) and EAW waves (SEAS) identified in the electrostatic spectrum at the same point in space (see figure 2).

electrons have been trapped and accelerated. A beam, similar to that observed in simulations of Raman forward scatter [15], forms in the electron distribution which is clearly visible in plots (Figure 4b). This beam could potentially support BAMs, however the beam velocity (at $v_p = 6.9vT_e$) is too high to explain the observed scattering. The trapping of electrons by the Langmuir waves driven through SRS evolves into a plateau in the electron distibution. This flattened region extends to low phase velocities, providing an environment in which low frequency plasma modes are able to grow and propagate. These low frequency modes are visible in the electrostatic field spectrum after the collapse of the initial SRS burst at $t \approx 600/\omega_{pe}$, and correspond to two distinct electron acoustic waves (eaw1 and eaw2) at $\omega_{eaw1} = 0.73\omega_{pe}$, $k = 0.27/\lambda_D$, $v_p = 2.73vT_e$, and later $\omega_{eaw2} = 0.57\omega_{pe}$, $k = 0.28/\lambda_D$.

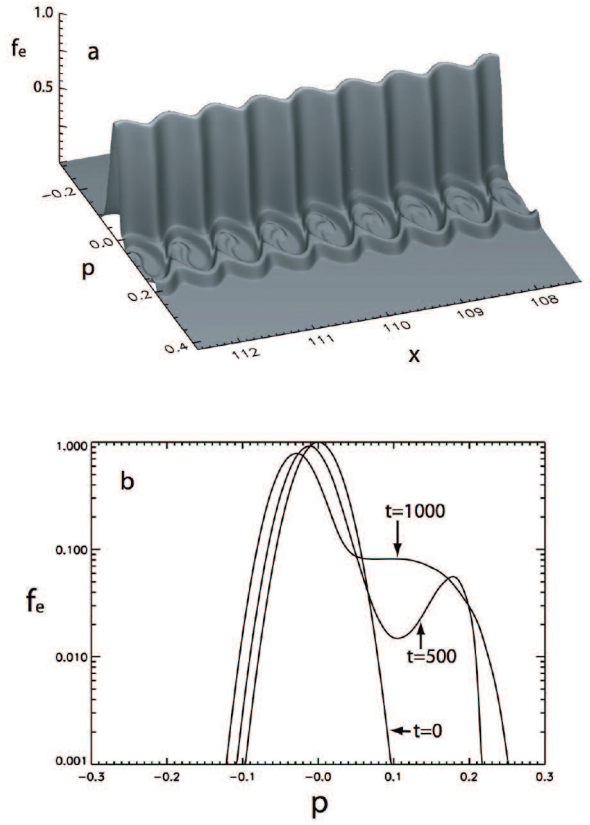

Figure 4. (a) Surface plot of the electron distribution near the centre of the system at $t = 500/\omega_{pe}$. Electron trapping, visible here, is responsible for the saturation of the Raman instability and the creation of the electron beam in the spatially integrated distribution. (b) Spatially integrated electron distribution functions, for $t = 0$, $t = 500/\omega_{pe}$ and $t = 1000/\omega_{pe}$ normalised to the initial Maxwellian distribution. The trapping of electrons in the Langmuir wave driven by SRS temporarily creates a beam structure. The collapse of this structure is responsible in part for the formation of a broad plateau in momentum space at late times, which supports EAWs.

The electron distribution at late times deviates significantly from a Maxwellian. The trapping of electrons in the initial SRS burst flattens the distribution around $p = 1.5m_ec$, allowing the development of low frequency plasma waves whose trapped electrons further distort the distribution of particles. By the simulation's end, it has become clear that the plasma, and hence the modes which it supports, is not well described by linear or fluid approximations. Scattering observed in single hot-spot experiments was from EAWs with phase velocity $v_p = 1.4v_{Te}$ ($k = 0.279/\lambda_D$, $\omega = 0.41\omega_{pe}$), with a backscattered wave amplitude over a thousand times smaller than that from SRS. The amplitude of EAWs, and of the light scattered from them, observed in simulations is greater than observed experimentally. The simulations outlined here also produce EAWs with higher phase velocities than the scattered spectra from experiments indicate. These two deviations are closely related. As shown earlier, the dispersion relation for the EAW is dictated in part by the mode amplitude. As the EAW amplitude is increased, the dispersion relation shifts inwards, as described in previous work [4], resulting in a higher phase velocity at fixed wavenumber. Further work is required to quantify in greater depth this inconsistency between numerical and experimental results.

The simulation runtime, $t = 1200/\omega_{pe}$, is equivalent to less than three picoseconds - this serves to highlight how rapid the switch from the fluid to the kinetic regime may be, at the laser intensities considered here. As laser intensity increases, the kinetic effects discussed here will become more critical to the understanding of the associated laser-plasma interaction physics.

Conclusions

Experiments studying fundamental laser-plasma interactions in a single hotspot [5,6] observed backscattered light from the interaction of the incident beam with two distinct plasma modes. First, there is scattering from waves having high phase velocity $v_p = 4.2v_{Te}$ and a frequency above the plasma frequency, which was attributed to SRS: the three-wave parametric instability involving a Langmuir wave. Second, there is scattering from waves of considerably lower phase velocity $v_p = 1.4v_{Te}$, whose frequency is below the plasma frequency. These low frequency modes were identified as the electron acoustic wave. The simulations reported here have attempted to model the key physics of this scattering using a 1D Vlasov-Maxwell approach. These have been successful in achieving scattering from both high and low frequency electron plasma waves (which we identify as Langmuir and electron acoustic waves respectively) but have not been able to reproduce exactly the phase velocities of the EAWs and the relative amplitudes of the scattering events.

Recent work [16-20] has identified the need for a deeper understanding of laser-plasma interactions, particularly in the regimes currently being approached by the next generation of lasers. The accurate noise-free representation and evolution of the particle distribution functions provided by a Vlasov code make it a valuable additional tool complementing both fluid and particle-in-cell descriptions. While a full 3D Vlasov treatment is beyond the limits of current computing power, 1D and 2D Vlasov systems are tractable and can address many relevant problems. The present study has indicated some of the distinctive features of the BAM, the EAW and associated physics that arise from a full kinetic treatment of the plasma.

Recent numerical work [21] has highlighted the possibility that 'trains' of electron holes, with low phase velocities, may be created by the action of a strong electrostatic driver

at a frequency above the plasma frequency. Such structures could become involved in scattering, and may be excited by the electrostatic daughter waves driven by the stimulated Raman and Brillouin instabilities. The interplay between the electrostatic mechanisms outlined by Califano *et al.*[21] and the electromagnetic scattering mechanism outlined here is a potentially interesting topic for future work.

References

1. A. Luque and H. Schamel. *Phys. Reports,* **415**, 261, (2005)
2. B. Afeyan, K. Won *et al.*, *"Proc. 3rd Int. Conf. on Inertial Fusion Sciences and Applications (Monterey, 2003)".* American Nuclear Society, **213**, (2004)
3. T. H. Stix.*"The Theory of Plasma Waves"* McGraw Hill (1962)
4. N. J. Sircombe, T. D. Arber and R. O. Dendy. *CLF Annual Report* (2005)
5. T. M. O'Neil and J. H. Malmberg. *Phys. Fluids,* **11**, 1754, (1968)
6. D. S. Montgomery, J. A. Cobble *et al.*, *Phys. Plasmas,* **9**, 2311, (2002)
7. D. S. Montgomery, R. J. Focia, H. A Rose *et al.*, *Phys. Rev. Lett.,* **87**, 155001, (2001)
8. L. Yin, W. Daughton *et al.*, *Phys. Rev. E,* **73**, 025401, (2006)
9. N. J. Sircombe, T. D. Arber and R. O. Dendy. *Plasma Phys. Control. Fusion,* **48**, 1141 (2006)
10. R. O. Dendy. *"Plasma Dynamics"* Oxford University Press (1990)
11. J. M. Grißmeier, A. Luque, and H. Schamel. *Phys. Plasmas*, **9**, 3816, (2002)
12. L. Nikolic, M. Skoric, S. Ishiguro, and T. Sato. *Phys. Rev. E,* **66**, 036404 (2002)
13. T. D. Arber and R. G. L. Vann *J. Comp. Phys.,* **180**, 339, (2002)
14. N. J. Sircombe, T. D. Arber and R. O. Dendy *Phys. Plasmas,* **12**, 012303, (2003)
15. A. Ghizzo, P. Bertrand, M. M. Shoucri *et al.*, *J. Comp. Phys.,* **90**, 431, (1990)
16. D. Pesme, S. Huller, J. Myatt *et al.*, *Plasma Phys. Control. Fusion,* **44**, B53, (2002)
17. C. Labaune, H. Bandulet, S. Depierreux *et al.*, *Plasma Phys. Control. Fusion,* **46**, B301, (2004)
18. S. H. Glenzer, P.Arnold, G. Bardsley *et al.*, *Nuclear Fusion,* **44**, (2004)
19. J. L. Kline, D. S. Montgomery, B. Bezzerides *et al.*, *Phys. Rev. Lett.,* **94**, 175003, (2005)
20. S. Weber, M. Lontano, M. Passoni *et al.*, *Phys. Plasmas,* **12**, 112107, (2005)
21. F. Califano and M. Lontano. *Phys. Rev. Lett.,* **95**, 245002, (2005)